A new role for the dynamin GTPase in the regulation of fusion pore expansion

Arun Anantharam[a], Mary A. Bittner[a], Rachel L. Aikman[a], Edward L. Stuenkel[b], Sandra L. Schmid[c], Daniel Axelrod[d], and Ronald W. Holz[a]

[a]Department of Pharmacology and [b]Department of Molecular and Integrative Physiology, University of Michigan, Ann Arbor, MI 48109; [c]Department of Cell Biology, The Scripps Research Institute, La Jolla, CA 92037; [d]Department of Physics and LSA Biophysics, University of Michigan, Ann Arbor, MI 48109

ABSTRACT **Dynamin is a master regulator of membrane fission in endocytosis. However, a function for dynamin immediately upon fusion has also been suspected from a variety of experiments that measured release of granule contents. The role of dynamin guanosine triphosphate hydrolase (GTPase) activity in controlling fusion pore expansion and postfusion granule membrane topology was investigated using polarization optics and total internal reflection fluorescence microscopy (pTIRFM) and amperometry. A dynamin-1 (Dyn1) mutant with increased GTPase activity resulted in transient deformations consistent with rapid fusion pore widening after exocytosis; a Dyn1 mutant with decreased activity slowed fusion pore widening by stabilizing postfusion granule membrane deformations. The experiments indicate that, in addition to its role in endocytosis, GTPase activity of dynamin regulates the rapidity of fusion pore expansion from tens of milliseconds to seconds after fusion. These findings expand the membrane-sculpting repertoire of dynamin to include the regulation of immediate postfusion events in exocytosis that control the rate of release of soluble granule contents.**

Monitoring Editor
Thomas F.J. Martin
University of Wisconsin

Received: Feb 4, 2011
Revised: Mar 22, 2011
Accepted: Mar 23, 2011

INTRODUCTION

A precisely orchestrated series of events underlie the proper execution of Ca^{2+}-triggered exocytosis and subsequent endocytosis in the chromaffin cell. These processes have classically been thought of as discrete and opposite, with unique proteins required for each, such as soluble N-ethylmaleimide-sensitive factor activating protein receptors (SNAREs) in exocytosis, and clathrin and adaptors in endocytosis. It has been believed that upon fusion the granule membrane rapidly collapses into the plasma membrane, where the granule membrane constituents await recycling by compensatory, clathrin-mediated endocytosis over many minutes. A growing body of evidence suggests that there are alternative pathways for recycling of the granule membrane (Artalejo *et al.*, 2002). Indeed, experiments have demonstrated that the fused granule is not obliged to flatten, but rather can be retrieved largely intact via a rapid form of endocytosis (Henkel and Almers, 1996) that does not require clathrin (Artalejo *et al.*, 1995). Rapid endocytosis can be distinguished kinetically from slower clathrin-mediated endocytosis by using capacitance measurements (Artalejo *et al.*, 2002) and with imaging techniques that assess the ability of a granule to release or take up fluorescent lumenal probes (Taraska *et al.*, 2003; Perrais *et al.*, 2004; Fulop *et al.*, 2005).

A protein that has emerged as the nexus between the exocytotic and endocytic arms of trafficking at the plasma membrane is the dynamin GTPase. Dynamin has an established role as a master controller of fission during endocytosis (Hinshaw and Schmid, 1995; Takei *et al.*, 1995). It forms rings or collars around the necks of budding endocytic vesicles (Hinshaw and Schmid, 1995), triggering cooperative GTP hydrolysis (Warnock *et al.*, 1996) and membrane remodeling, leading to fission (for recent reviews, see Doherty and McMahon, 2009, and Pucadyil and Schmid, 2009). A number of electrophysiological and amperometric studies suggest that

This article was published online ahead of print in MBoC in Press (http://www.molbiolcell.org/cgi/doi/10.1091/mbc.E11-02-0101) on April 1, 2011.

Address correspondence to: Arun Anantharam (arunanan@umich.edu), Ronald W. Holz (holz@umich.edu).

Abbreviations used: A.F.U., arbitrary fluorescence units; dil, 1,1′-dioctadecyl-3,3,3′,3′-tetramethylindocarbocyanine perchlorate, Dyn1; dynamin-1; GTPase, guanosine triphosphate hydrolase, HA, hemagglutinin; IgG, immunoglobulin G; NA, numerical aperture; NPY-Cer, neuropeptide Y-Cerulean; pHL, pHluorin; p-pol, p-polarized; PRD, proline-rich domain; *P/S*, (p-pol emission)/(s-pol emission); *P* + *2S*, p-pol emission + 2(s-pol emission); PSF, prespike foot; PSS, physiological salt solution; pTIRFM, polarization optics and total internal reflection fluorescence microscopy; ROI, region of interest; SNAP25, synaptosomal-associated protein 25; SNARE, soluble N-ethylmaleimide-sensitive factor activating protein receptor; s-pol, s-polarization; VMAT2-pHL, vesicular monoamine transporter 2–pHL; WT, wild-type.

dynamin can function not only in endocytosis but also immediately upon fusion to regulate the kinetics of granule content release (Graham *et al.*, 2002; Holroyd *et al.*, 2002; Tsuboi *et al.*, 2004; Fulop *et al.*, 2008; Gonzalez-Jamett *et al.*, 2010) and membrane protein dispersal into the plasma membrane (Jaiswal *et al.*, 2009). Since dynamin has a proclivity for highly curved membrane structures that occur upon fusion, it could be playing a heretofore unsuspected role in fusion pore expansion immediately upon, or soon after, fusion. Indeed, in a recent study in which we combined polarization optics and TIRFM (pTIRFM) to directly detect membrane topological changes of the expanding fusion pore (Anantharam *et al.*, 2010b), we found that dynasore, a putative inhibitor of dynamin function in situ (Macia *et al.*, 2006), slowed the kinetics and altered the characteristics of the membrane changes.

The GTPase activity of dynamin plays a critical role in catalyzing membrane fission in endocytosis. Mutants that alter the GTPase activity alter the rates of clathrin-mediated endocytosis. In the following study, we ask a specific question: does dynamin GTPase activity regulate fusion pore expansion? Rather than use pharmacological agents, peptide blockers, or antibodies to modulate dynamin function, adrenal chromaffin cells were transfected to transiently express wild-type dynamin-1 (Dyn1WT), dynamin-1 mutant T65A (Dyn1(T65A)) with reduced GTPase activity, or dynamin-1 mutant T141A (Dyn1(T141A)) with elevated GTPase activity (Marks *et al.*, 2001; Song *et al.*, 2004). Two methods were used to assess the outcome of the fusion event: polarization optics and TIRFM (pTIRFM) and amperometry. pTIRFM was used to directly image the granule membrane/plasma membrane domain. We have recently refined this technique to be able to measure membrane deformations with submicron spatial and 100 ms temporal resolution. We used amperometry to assess fusion pore expansion within milliseconds of fusion by measuring the kinetics of catecholamine release from individual fusion events.

We find that when dynamin GTPase activity is reduced, expansion of the fusion pore is slowed with concomitant long-lasting membrane deformations. When dynamin GTPase activity is elevated, fusion pore expansion is accelerated, with more rapid curvature transitions. The ability to identify specific effects of the GTPase activity directly demonstrates a role for dynamin in secretion and suggests a mechanism that may explain its function. The findings expand the membrane-sculpting repertoire of dynamin to include the regulation of immediate postfusion events in exocytosis.

RESULTS

Extent of rapid endocytosis is coupled to Dyn1 GTPase activity

Because the dynamin GTPase mutants used in the study have not been investigated in primary secretory cells, we first explored their effects on the frequency of individual endocytic events that immediately follow exocytosis at sites of fusion. A method that is based upon the granule marker, VMAT2, labeled with the highly pH-sensitive fluorophore, pHluorin (pHL; Anantharam *et al.*, 2010b; Onoa *et al.*, 2010) was used. Bovine adrenal chromaffin cells expressing VMAT2-pHL were exposed to a cycle of pH 5.5 and pH 7.4 for 10 s after an initial 15-s stimulation with 56 mM K^+ in the presence of bafilomycin. The low extracellular pH quenches surface pHL but not pHL that has undergone endocytosis. Endocytic events (i.e., events insensitive to low-pH quench) were tabulated and the results are shown in Figure S1. In cells expressing VMAT2-pHL alone, 17% of fusion events are followed by rapid endocytosis. When Dyn1WT is coexpressed in the cells, there is little change in this frequency (15%). Dyn1(T65A) with greatly reduced GTPase activity and reduced GTP affinity decreased the frequency to 7%, whereas Dyn1(T141A) with increased GTPase activity increased the frequency to 22%. The effects of the GTPase mutants on rapid endocytosis are similar to those for slow, clathrin-mediated endocytosis in HeLa cells in which Dyn1(T65A) slows and Dyn1(T141A) enhances transferrin internalization (Song *et al.*, 2004). Notably, the vast majority of elevated K^+-stimulated fusion events, with or without transfected dynamin mutants, was not associated with endocytosis within 15 s.

The use of polarized-TIRFM to monitor localized membrane topological changes at the sites of fusion

We had previously demonstrated that membrane topological changes at the site of granule fusion could be reliably detected in bovine adrenal chromaffin cells by polarized excitation of 1,1′-dioctadecyl-3,3,3′,3′-tetramethylindocarbocyanine perchlorate (dil) in the plasma membrane using TIRFM (Anantharam *et al.*, 2010b). For the present experiments, cells were cotransfected with neuropeptide Y-Cerulean (NPY-Cer, sorted to the granule lumen) and various Dyn1 constructs to investigate the involvement of this protein in regulating postfusion topological changes at the sites of exocytosis. The plasma membrane was labeled with dil (Anantharam *et al.*, 2010b), and cells were stimulated to secrete with elevated K^+ (56 mM) for 60 s. Images needed to report membrane deformation were obtained by repeated sequences (10 Hz sequence frequency) of three TIR excitations: 442 nm (to obtain the NPY-Cer image); s-polarized (s-pol) 514 nm (perpendicular to the plane of incidence and parallel to the coverslip, to obtain the dil "s" image), and p-polarized (p-pol) 514 nm (in the plane of incidence and perpendicular to the coverslip, to obtain the dil "p" image). Figure S2 shows an example of the images from a fusion event.

The image ratio *P/S* reports local membrane deviations from parallelism with the glass coverslip. Any membrane deformation that changes the orientation of the plasma membrane from planar will increase *P/S*. The amplitude of the increase of *P/S* can be predicted by computer simulations (Anantharam *et al.*, 2010b), which show it is quite sensitive even to small deformations. Therefore, *P/S* is the main parameter used here to detect and follow membrane deformations.

In our previous studies (Anantharam *et al.*, 2010a, 2010b), changes in *P/S* occurred within 0.5 s of the release of lumenal granule protein (the time resolution of the experiments), decayed with variable time courses from less than a second to many tens of seconds, and were kinetically distinct from endocytosis. dil rapidly diffused into the granule membrane from the plasma membrane upon fusion, and topological changes were detected reflecting intermediate and late stages of fusion pore expansion. Significantly, topological changes were altered when dynasore (Newton *et al.*, 2006; Macia *et al.*, 2006), a putative inhibitor of dynamin GTPase activity, was applied to cells.

The linear combination *P + 2S* approximately reports total dil emission from that location, which, in theory, is proportional to the amount of dil at any x-y-z location convolved with the evanescent field intensity, which decays exponentially with z distance from the coverslip. (The approximation is valid if the collection efficiency of the objective is fairly insensitive to emission polarization over the whole range of z distances, as it is for high-aperture objectives such as the numerical aperture [NA] 1.49 [Anantharam *et al.*, 2010b].) The interpretation of changes in *P + 2S* in terms of geometrical models is more ambiguous than for *P/S*, with increases, decreases, or no detectable change possible, depending upon various countervailing tendencies arising from geometrical details. Computer simulations (Anantharam *et al.*, 2010b) indicate that *P + 2S* will increase if

the geometry results in more dil-labeled membrane close to the glass interface. *P + 2S* decreases if dil diffuses into a postfusion membrane indentation (placing dil farther from the substrate, and thereby in a dimmer evanescent field intensity), or if there is less dil close to the substrate in the region of interest (e.g., if dil diffusion into a fused granule membrane is slowed by diffusion barriers).

Effects of transfected Dyn1WT on plasma membrane deformations associated with exocytosis

We first investigated the effects of transiently expressed Dyn1WT on membrane topological changes following granule fusion in bovine adrenal chromaffin cells. Membrane deformations (increases in *P/S*) were observed within 100 ms of NPY-Cer release in 87% of the fusion events in cells with and without transfected Dyn1WT. Fusions without evident changes in *P/S* probably reflect transient topological changes that occurred faster than the temporal resolution of the technique. An example of the change in *P/S* upon NPY-Cer release in a cell expressing Dyn1WT is shown in Figure 1A and quantitated in Figure 1B (a control example is shown in Figure 1C). The increase in *P/S* was maximal within 0.2 s of NPY-Cer release and rapidly decayed.

The most significant effect of overexpressed Dyn1WT on membrane topology was the speedier return of *P/S* back to baseline after fusion. This effect is evident in cumulative histograms of *P/S* changes for the population of events without (control) and with transfected Dyn1WT at different times after fusion (Figure 1D). The cumulative histograms were similar for the two groups at 0.2 s. However, by 5 s, the shift to lower values was greater for Dyn1WT, indicating a faster decay to baseline ($p < 0.05$, Mann–Whitney test).

The spectrum of *P + 2S* changes was not significantly different between the groups. *P + 2S* increases were detected in 7 out of 29 fusion events (8 cells) in the control group and in 9 out of 23 events (5 cells) in the Dyn1WT group. *P + 2S* decreases were detected in 7 out of 29 events in the control group and 3 out of 23 events in the Dyn1WT group. This variability is consistent with computer simulations (Anantharam *et al.*, 2010b), which indicate sensitivity of *P + 2S* to the exact geometry of the membrane deformation. Increases in *P + 2S* might reflect the presence of additional dil-labeled membrane at the fusion site, such as for a dil-labeled fused granule connected to the dil-labeled plasma membrane by a short neck that is narrower than the granule diameter. Conversely, decreases in *P + 2S* might reflect decreased excitation of dil due to the exponentially decaying evanescent field in more distal parts of an invagination, such as for a partially collapsed granule.

The following experiments compare expression of Dyn1 GTPase mutants with transfected Dyn1WT.

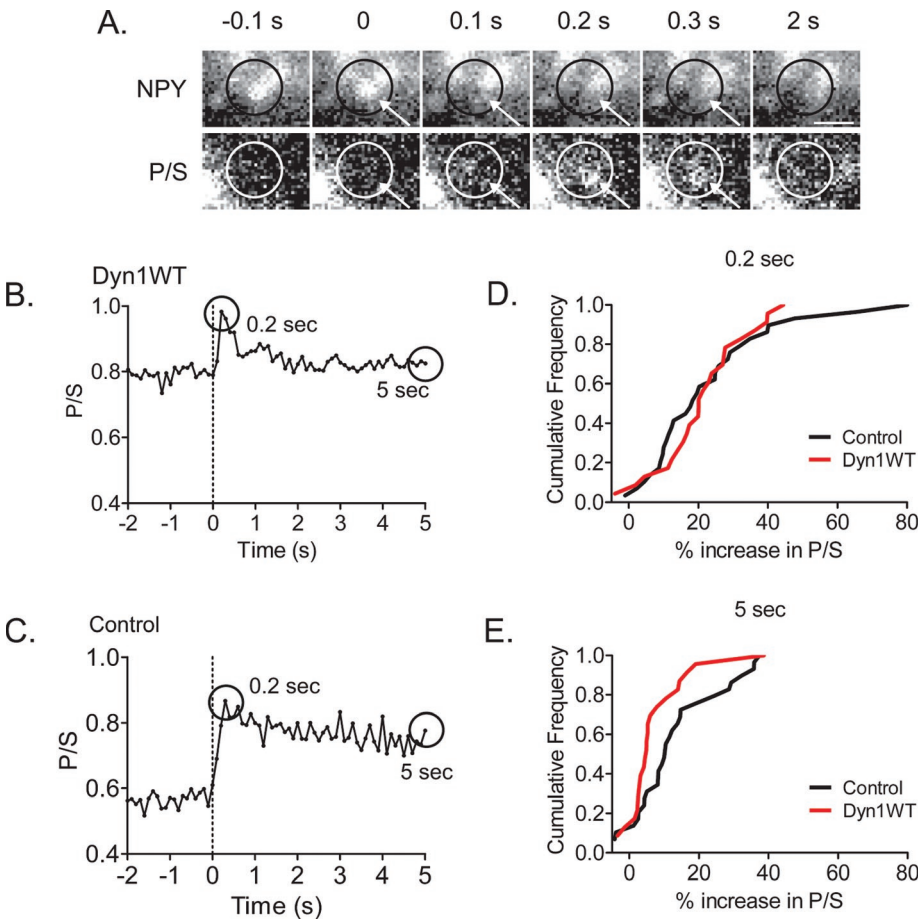

FIGURE 1: Membrane deformations at the sites of granule fusion are more transient in cells with transfected Dyn1WT than without (control). (A) Images are shown of pTIRFM responses (*P/S*) to exocytosis in a cell with transfected human Dyn1WT. Circles and arrows highlight the region of the transient *P/S* increase. Scale bar: 1 µm. (B) The *P/S* intensity from A is depicted in the graph. The dotted line indicates the frame before fusion of the NPY-Cer–labeled granule. (C) An example of the *P/S* response in a control (no transfected dynamin) cell is shown. (D) Cumulative frequency histograms were generated to compare the dynamics of the *P/S* change observed at 0.2 and 5 s (*P/S* at these times is circled in graphs shown in B and C) in cells without and with transfected Dyn1WT. Percent increases for individual events were calculated by taking the difference between the *P/S* at indicated times after granule fusion $(P/S)_f$ and the average *P/S* of 20 pre-fusion frames (Ave_{pre}), divided by the average; $[(P/S)_f - Ave_{pre}]/ Ave_{pre}$. At 0.2 s, the same proportion of fusion events (87%) were associated with a significant increase in *P/S*. By 5 s, the *P/S* change had declined to baseline in a greater proportion of events from cells transfected with Dyn1WT than control. Dyn1WT, n = 23 events from 5 cells. Control, n = 29 events from 8 cells. The two groups are significantly different at 5 s ($p < 0.05$, Mann–Whitney test).

The topological fate of the granule membrane after fusion is regulated by Dyn1 GTPase activity

Expression of Dyn1 mutants with either decreased (T65A) or increased (T141A) GTPase activity substantially altered the topological changes detected upon fusion compared with Dyn1WT. The effects of the mutants could be distinguished both by the time course of the membrane deformations (*P/S*) and their possible geometries (as suggested by changes in *P + 2S*). Representative examples of *P/S* and *P + 2S* changes in cells expressing the mutants are shown in Figure 2. In a cell expressing Dyn1(T65A), the increase in *P/S* was long-lived and associated with an increase in *P + 2S* (Figure 2, A and B). In a cell expressing Dyn(T141A), the increase in *P/S* was short-lived and associated with a decrease in *P + 2S* (Figure 2, D and E).

These tendencies were evident in the population of responses. The membrane deformations (*P/S*) upon fusion in cells expressing Dyn1(T65A) were long-lived, with

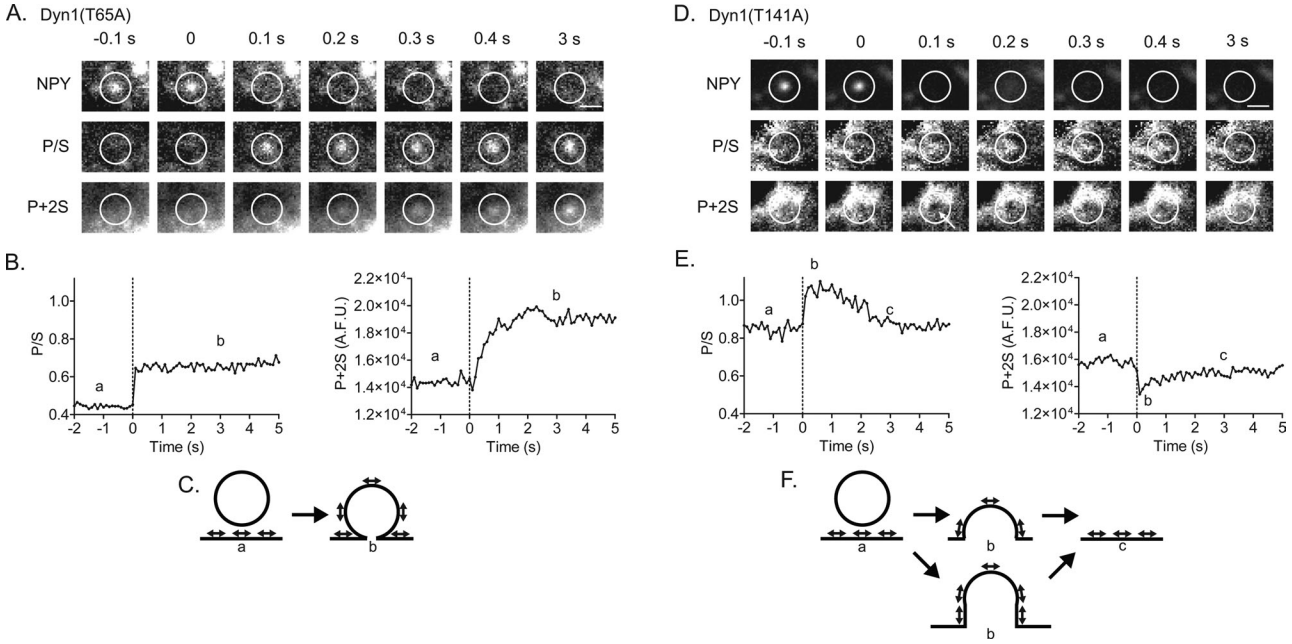

FIGURE 2: Examples of membrane topological changes after fusion in cells expressing Dyn1 GTPase mutants. Chromaffin cells were cotransfected with NPY-Cer and either Dyn1(T65A) or Dyn1(T141A). (A) Images are shown of pTIRFM responses (*P/S* and *P + 2S*) to exocytosis in a cell with transfected human Dyn1(T65A). (B) The *P/S* and *P + 2S* increase is long-lived in a cell transfected with Dyn1(T65A) with low GTPase activity. (C) One interpretation of the event is considered in the cartoon. The data are also consistent with a dil-labeled granule having undergone endocytosis at the site of fusion and remaining close to the plasma membrane (not shown). dil transition dipole moment orientation is indicated by direction of arrowheads. (D, E) Conversely, the *P/S* increase after fusion is transient in a cell transfected with Dyn1(T141A) with elevated GTPase activity. *P + 2S* transiently decreases in region highlighted by white arrow (D). (F) The changes observed are consistent with computer simulations of structures shown in the cartoon. Another possibility not shown is rapid endocytosis with retreat of the dil-labeled granule into the cell.

little change in cumulative histograms at different times after NPY-Cer release (Figure 3A). This is in contrast to the shift to the left (to smaller *P/S*) for cells expressing Dyn1WT and Dyn1(T141A). Furthermore, in the presence of Dyn1(T141A), 45% of the fusion events were not associated with a change in *P/S* compared with 13% in control cells, 13% in cells expressing Dyn1WT, and 0% in cells expressing Dyn1(T65A). The increased incidence of fusion events without evident changes in *P/S* in cells expressing Dyn1(T141A) probably reflects topological changes occurring faster than the temporal resolution of the technique.

The distributions of *P/S* changes in the mutants were also directly compared with Dyn1WT. Dyn1(T65A) with greatly reduced GTPase activity prolonged the membrane deformations associated with fusion (Figure 3B, right panel). Deformations are more transient in cells with Dyn1(T141A) with increased GTPase activity (Figure 3B, left panel; cumulative histograms shift to the left).

The different GTPase mutants not only changed the dynamics of the membrane deformations (*P/S*), but also caused differences in the total dil emission (*P + 2S*), suggestive of different geometries. In cells expressing Dyn1(T65A), *P + 2S* increased in 16 of 23 fusion events (Figure 2B, right panel and Figure 3C). There were no decreases. The increases tended to be larger and longer lasting than in cells expressing Dyn1WT. In contrast, in cells expressing Dyn1(T141A), *P + 2S* tended to decrease (Figure 2E, right panel) or remain unchanged, with only one increase in *P + 2S* in 29 fusion events (Figure 3C).

Computer simulations can guide us in the interpretation of *P/S* and *P + 2S* changes. The long-lived deformation with additional dil-labeled membrane (i.e., increased *P + 2S*; Figure 3C) in cells expressing Dyn1(T65A) is consistent with a granule membrane connected to a plasma membrane via a short neck. This would occur if expansion of the pore is limited after fusion (Figure 2C). Long-lived increases in *P/S* and *P + 2S* might also result from a dil-labeled granule undergoing endocytosis but remaining close to the plasma membrane. However, this outcome is unlikely given the lower frequency of endocytosis with Dyn1(T65A) [Figure S1 and Song *et al.*, (2004)]. Conversely, in cells expressing Dyn1(T141A), deformations (*P/S*) after fusion are transient and are usually accompanied by decreases, rather than increases, in *P + 2S*. These changes suggest that expansion of the pore accelerates after fusion, resulting in substantial or complete collapse of the granule membrane into the plasma membrane (Figure 2F). This interpretation is also consistent with the amperometric data in the next section.

We also investigated whether expression of dynamin GTPase mutants altered the speed of NPY-Cer release. In cells without overexpressed dynamin or with overexpressed Dyn1WT, complete NPY-Cer release required greater than 200 ms in only 13.5% (5/37) or 11% (2/27) of the events, respectively. In cells expressing Dyn1(T65A), the fraction increased to 30% (8/29, $p < 0.05$ vs. Dyn1WT), whereas in cells expressing Dyn1(T141A), the fraction was 6% (2/32, not significantly different from Dyn1WT). We conclude from these data that the longer-lived deformations in the presence of Dyn1(T65A) restrict protein release, consistent with the occurrence of a narrow fusion neck. These findings are similar to those of Tsuboi *et al.* (2004), who used a different vesicle content protein and a different set of Dyn1 protein mutants in PC12 cells.

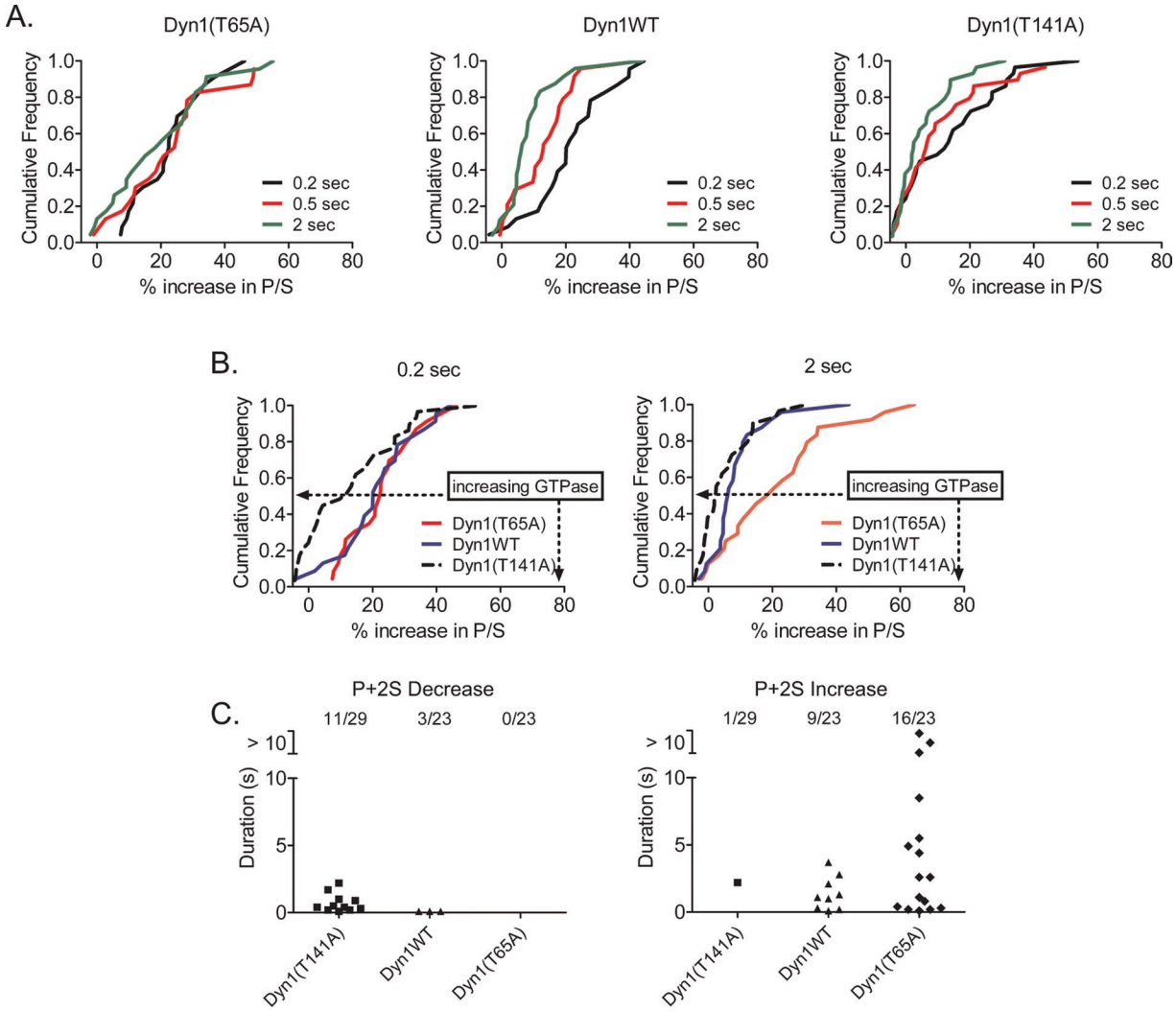

FIGURE 3: Dyn1 GTPase activity regulates the dynamics of membrane deformations after fusion. (A) Cumulative frequency histograms were generated to compare the dynamics of the *P/S* change observed at 0.2, 0.5, and 2 s in cells transfected with Dyn1(T65A), Dyn1(T141A), and Dyn1WT. For Dyn1WT and Dyn1(T141A), the distribution of *P/S* changes at 0.5 and 2 s are significantly different ($p < 0.01$, Wilcoxon matched-pairs test) from the distribution at 0.2 s. The distribution of *P/S* changes at 0.5 and 2 s is not significantly different from the distribution at 0.2 s for Dyn1(T65A). (B) The *P/S* increase remaining after 0.2 and 2 s postfusion is shown in the cumulative histogram. At 0.2 s, Dyn1(T141A) is significantly different from Dyn1WT ($p < 0.05$, Mann–Whitney test); Dyn1(T65A) is not significantly different from Dyn1WT. At 2 s, Dyn1(T141A) is not significantly different from Dyn1WT; Dyn1(T65A) is significantly different from Dyn1WT ($p < 0.01$, Mann–Whitney test). Dyn1(T65A), n = 23 events from 7 cells; Dyn1(T141A), n = 29 events from 6 cells. (C) The duration of *P + 2S* changes. Each data point represents an individual event. The number of decreases or increases in *P + 2S* was tabulated for each group as indicated in the cumulative histogram (e.g., *P + 2S* decreased after 11 out of 29 total fusion events for Dyn1(T141A), and 3 out of 23 total fusion events for Dyn1WT).

Dyn1 GTPase activity regulates early fusion pore expansion

The membrane events detected by pTIRFM are associated with intermediate and late fusion pore expansion. To address the possibility that the dynamin GTPase activity regulates fusion pore expansion within milliseconds of exocytosis, carbon-fiber amperometry was performed to measure the dynamics of catecholamine release from chromaffin granules. Most of the catecholamine release during an individual fusion event is accounted for by the amperometric current spike, which reflects rapid transmitter release through a fusion pore that has already partially widened (Wightman *et al.*, 1991; Chow *et al.*, 1992; Zhou *et al.*, 1996). The pre-spike foot (PSF) reflects catecholamine released through an initial narrow fusion pore (Albillos *et al.*, 1997). Figure 4A shows an example of an amperometric spike with a long PSF. Expression of Dyn1WT in chromaffin cells had no effect on the percentage of spikes detected with a PSF compared with the control group (Figure 4B). Expression of Dyn1(T141A) with increased GTPase activity significantly reduced the percentage of spikes with a PSF from 46% for Dyn1WT to 34% (Figure 4B; $p < 0.05$, Student's unpaired *t* test). Transfection of Dyn1WT and Dyn1(T141A) also affected the duration of the PSF. Following the methodology of Jackson and colleagues (Wang *et al.*, 2001), we calculated that the foot duration (τ) in control cells was 11.93 ± 0.14 ms. In cells expressing Dyn1WT, foot duration shortened significantly to 8.81 ± 0.12 ms.

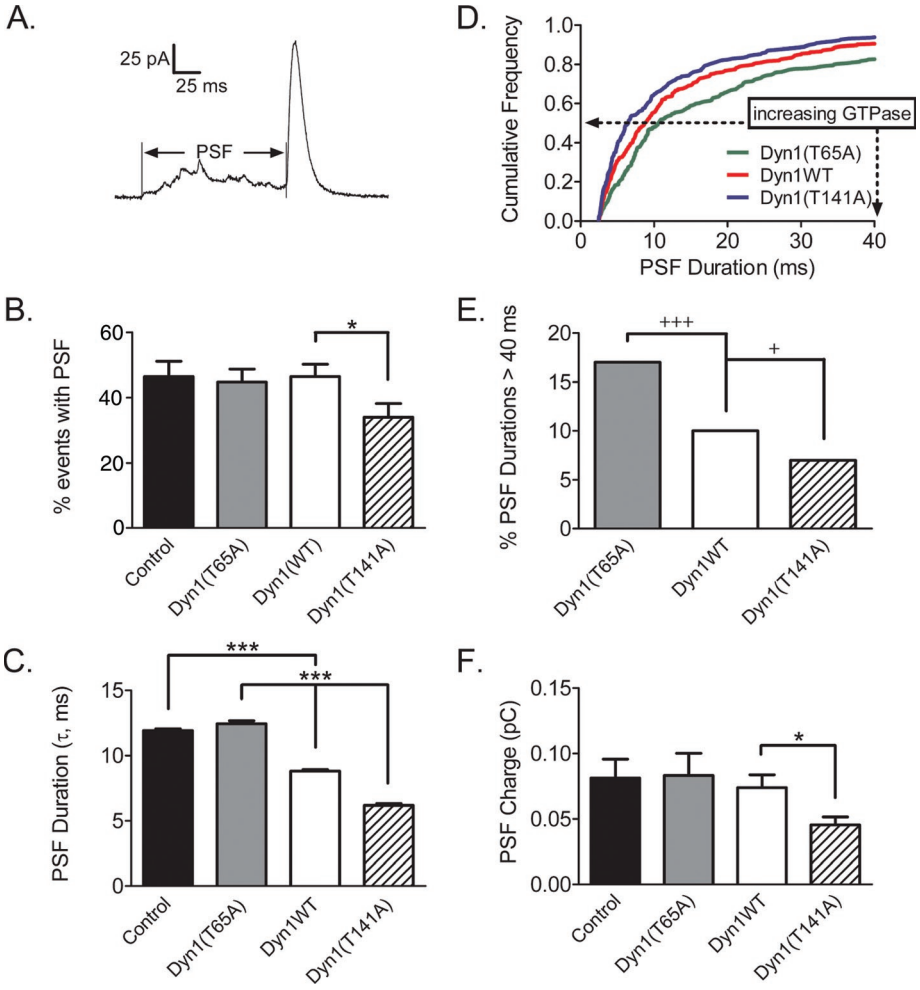

FIGURE 4: Amperometry of individual catecholamine release events indicates that Dyn1 GTPase activity regulates early fusion pore expansion. (A) An example of an amperometric spike with a long PSF. (B) The average frequency of spike events preceded by a PSF in a cell. Spikes: control, n = 601/37 cells; Dyn1WT, n = 594/43 cells; Dyn1(T141A), n = 720/45cells; Dyn1(T65A), n = 588/33 cells. Control is not significantly different from Dyn1WT. Dyn1(T65A) is not significantly different from Dyn1WT (*$p < 0.05$, Student's *t* test). Dyn1(T141A) is significantly different from Dyn1WT. (C) PSF durations (τ) were calculated as described in *Materials and Methods* (***$p < 0.001$, Student's *t* test). (D) Relative cumulative histogram of PSF durations for Dyn1WT and mutants. (E) The fraction of PSFs with durations greater than 40 ms ($^{+}p < 0.05$,$^{+++}p < 0.001$, test of binomial probability). (F) Median charge released during PSF (*$p < 0.05$, Student's *t* test). No significant differences found between control and Dyn1WT or between Dyn1(T65A) and Dyn1WT.

Transfection of Dyn1(T141A) with elevated GTPase activity further shortened the foot duration to 6.19 ± 0.14 ms (Figure 4C). The total amount of PSF charge (proportional to the amount of released catecholamine) was also reduced, from 0.074 ± 0.010 pC for WT to 0.045 ± 0.006 pC (Figure 4F). Note that these changes occurred without affecting quantal size (Figure S3A), indicating that Dyn1(T141A) specifically hastened the initial fusion pore expansion.

Dyn1(T65A), with low GTPase activity, prolonged the foot duration to 12.45 ± 0.22 ms compared with Dyn1WT (8.81 ± 0.12 ms; Figure 4C). Further analysis revealed that the mutant significantly increased the fraction of PSFs with relatively long durations (Figure 4, D and E). For example, 17% of the PSFs were longer than 40 ms in cells expressing Dyn1(T65A) compared with 10% for cells overexpressing Dyn1WT, indicating that the mutant tended to slow fusion pore expansion.

Imaging of chromaffin cells shows that Dyn1 expression is punctate and primarily localized to the plasma membrane

The effects of transfected Dyn1 and Dyn1 GTPase mutants on early (amperometry) and later (pTIRFM) fusion pore expansion, suggested that the protein must already be present at, or rapidly recruited to, sites of exocytosis. To investigate this issue, we performed immunocytochemical staining of dynamin in chromaffin cells transfected either with NPY-Cherry alone (to visualize granules), or together with Dyn1WT, Dyn1(T65A), or Dyn1(T141A). Transfected Dyn1 proteins were visualized with an antibody (Hudy 1) that recognizes the proline-rich domain (PRD) of Dyn1 (Damke *et al.*, 1994; Warnock *et al.*, 1995). The antibody also recognizes Dyn2 (Warnock *et al.*, 1997). In unstimulated cells, endogenous dynamin was largely localized to the plasma membrane as puncta (Figure 5A, left panel). In cells transfected with Dyn1WT or Dyn1(T65A) (Figure 5, B and C), the protein was still primarily localized to the plasma membrane with a predominantly punctate appearance. Dyn1(T141A)-expressing cells had a similar appearance (unpublished data). The amount of dynamin on the plasma membrane in dynamin-transfected cells was increased 2.5 to 3.5 times compared with endogenous dynamin in cells transfected with NPY-Cherry alone (Figure S4A). There was also increased expression in the cell interior in dynamin-transfected cells (Figure S4B).

Next the spatial relationship of peripheral secretory granules and dynamin was evaluated. NPY granules were often in close proximity to dynamin puncta on the plasma membrane (center of intensities within 200 nm; Figure 5, white arrows). However, overlap of granules with dynamin puncta (center of intensities separated less than 70 nm) was rare, with the most frequently occurring overlap in cells expressing Dyn1(T65A) (Figure 5C, yellow arrows). The frequency of overlap for the various expression conditions is presented in Figure 6, and ranged from 1.5% for overlap with endogenous dynamin to 10% with Dyn1(T65A). Although it is possible that some of the overlap is random, the decreasing frequency of overlap with increasing GTPase activity suggests a rare but specific interaction that is regulated by the GTPase activity. In sum, confocal, immunocytochemical studies demonstrate that although exact colocalization with granules is rare, Dyn1 is primarily found on the plasma membrane, where it is close to granules and to likely sites of exocytosis.

To determine whether Dyn1 puncta are favored sites of exocytosis, and whether Dyn1 rapidly accumulates at sites of granule fusion, TIRFM studies were performed in cells cotransfected with NPY-Cherry (to visualize granules), and Dyn1WT- or Dyn1(T65A)-GFP (to visualize transfected Dyn1). The dynamin construct used in these studies has been previously reported to be functional in cells (Liu

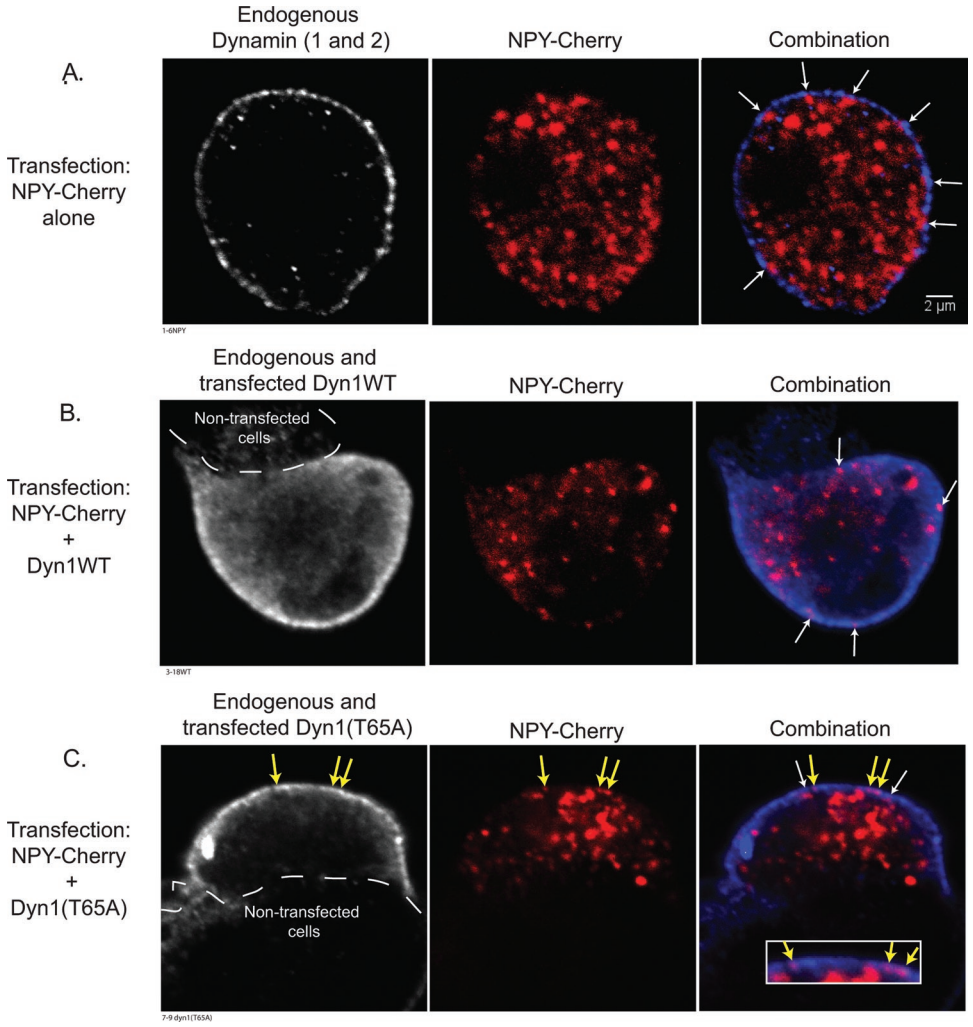

FIGURE 5: Confocal imaging of chromaffin cells shows Dyn1 expression to be punctate and primarily localized to the plasma membrane. Chromaffin cells cultured on glass coverslips were transfected with a plasmid encoding NPY-Cherry alone (A), with a plasmid encoding Dyn1WT (B), or with a plasmid encoding Dyn1(T65A) (C). Four or five days after transfection, cells were fixed, permeabilized, and exposed to the Hudy 1 antibody, which recognizes an epitope within the PRD of dynamin. Confocal sections were taken through the center of the cells of interest. Dyn1 is colored blue in the combination. White arrows indicate examples of secretory granules that are in close apposition but not coinciding with dynamin puncta (center of intensities separated by greater than 70 nm). Yellow arrows in (C) indicate granules that overlap with dynamin puncta (center of intensities within 70 nm). Inset in combination in (C) shows higher magnification of area above, with white arrows omitted. Areas of the cell membrane abutting other cells did not stain as well for Dyn1 as those exposed to the extracellular medium (B, C, dashed line indicating outline of neighboring nontransfected cell).

et al., 2008). Dyn1-GFP expression at the TIR-interface was mostly punctate, with some diffuse fluorescence visible (Figure 7, A and B). This is similar to the immunocytochemistry in Figure 5. Puncta only rarely colocalized with granules (4.8% colocalization was detected for Dyn1WT and 7% for Dyn1(T65A)). There was no tendency for granules to fuse at sites of Dyn1WT puncta upon stimulation, and there was no evidence for accumulation of Dyn1WT at sites of granule fusion. If Dyn1 accumulation precedes or accompanies granule fusion, we reasoned that it may be more apparent when GTPase activity is slowed. However, accumulation was not detected, even when Dyn1(T65A)-GFP was used. We did observe that a local decrease in dynamin fluorescence frequently occurred immediately following fusion (Figure 7, C and D). It is likely that Dyn1-GFP was present locally before fusion, and subsequently either was excluded from the area by the fused granule/plasma membrane structure or diffused into the fused granule membrane that retained curvature in the decaying evanescent field. This phenomenon has been observed with another membrane-targeted fluorescent protein, synaptosomal-associated protein 25 (SNAP25(1–100); Figure S5), which is inactive in secretion (Wang *et al.*, 2008).

Atomic force microscopy does not reveal a change in surface elasticity due to expression of Dyn1(T65A)

Membrane tension is likely to be an important factor in fusion pore expansion. Because there is evidence in vitro that dynamin can induce membrane tension in the presence of GTP (Roux *et al.*, 2006), we investigated the possibility that changes in fusion pore expansion were caused by a global change in membrane tension

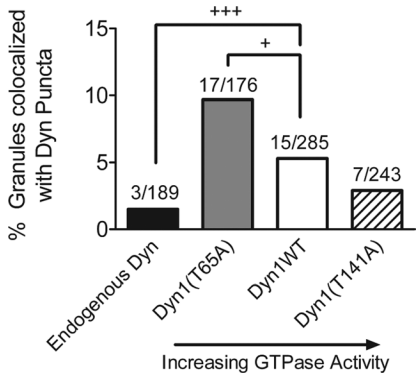

FIGURE 6: Colocalization of granules with Dyn1 puncta. The percentage of granules showing overlapping expression with Dyn1 puncta (center of intensities within 70 nm, as shown in yellow arrows in Figure 5) is indicated for endogenous (Dyn1 and Dyn2) and transfected Dyn1. Numbers above columns indicate number of overlapping granules and dynamin puncta/total number of granules analyzed (8–12 cells/group; $^{+}p < 0.05$,$^{+++}p < 0.001$, test of binomial probability).

caused by overexpression of dynamin mutants. Atomic force microscopy was used to directly measure surface elasticity of chromaffin cells with and without transfected Dyn1(T65A). The deflection of a 20-nm diameter probe at the end of a cantilever with a low spring constant was measured as it was lowered against the surface of nontransfected cells or cells expressing Dyn1(T65A) (Figure 8, representative traces). There was little difference in the initial slopes of the probe deflection upon approach to the cells. The initial slopes for nontransfected and Dyn1(T65A)-expressing cells were 0.055 ± 0.008 nm/μm (32 measurements from 4 cells) and 0.061 ± 0.007 nm/μm (37 measurements from 5 cells), respectively. Approach to a plastic surface resulted in an initial slope ~20 times greater, representing almost zero elasticity. Thus, it is unlikely that the slower expansion of the fusion pore upon expression of Dyn1(T65A) was caused by generalized change in the surface tension.

DISCUSSION

We have investigated whether dynamin, which can shape biological membranes and plays a central role in membrane fission in endocytosis, also plays a role in shaping the granule membrane/plasma membrane domain that results from fusion in neuroendocrine cells. Two independent techniques were used to investigate individual fusion events in bovine adrenal chromaffin cells. Amperometry measured the dynamics of catecholamine release from milliseconds to 100 ms after fusion, and pTIRFM measured membrane deformations from 100 ms to many seconds after fusion. Thus, for the first time, the full time course of changes was investigated, from the initial fusion pore to later outcomes.

A number of studies suggested that dynamin can function not only in endocytosis, but also immediately upon fusion, to regulate the kinetics of granule content release (Graham *et al.*, 2002; Holroyd *et al.*, 2002; Tsuboi *et al.*, 2004; Fulop *et al.*, 2008; Anantharam *et al.*, 2010b; Gonzalez-Jamett *et al.*, 2010) and membrane protein dispersal into the plasma membrane (Jaiswal *et al.*, 2009). In this study, we limited ourselves to a specific question based upon the importance of GTP hydrolysis in dynamin function in endocytosis: what are the effects of dynamin mutants with different GTPase activities on fusion pore expansion? We draw two major conclusions from our study: 1) Dynamin exerts GTPase-dependent effects on fusion pore expansion within milliseconds of granule fusion; 2) The GTPase activity of dynamin regulates the topological fate of the granule membrane after fusion (i.e., collapse, maintained curvature, or rapid endocytosis).

Dynamin GTPase activity regulates fusion pore expansion

Dyn1 mutants with differing GTPase activities were transiently expressed in chromaffin cells (Figures 2–4). The effects of these mutants on exocytosis were remarkably self-consistent. A mutant with greatly reduced GTPase activity, Dyn1(T65A), slowed expansion of the fusion pore, and slowed protein release, with long-lasting membrane deformations (longer PSF lifetimes and longer-lived *P/S* changes). A mutant with elevated GTPase activity, Dyn1(T141A), hastened fusion pore expansion, with more transient deformations. In fact, for this mutant, membrane deformations were so rapid that they were not detected following almost half of the fusion events.

Dynamin is able to exert rapid effects upon secretion because it is already at or close to fusion sites

Immunocytochemical analysis shows that endogenous dynamin is highly concentrated along the plasma membrane, labeling most of the exposed membrane (Figure 5A). The overexpressed protein is either associated with the plasma membrane (usually as puncta) or is in the immediately adjacent cytoplasm (Figure 5B). TIRFM imaging of chromaffin cells also revealed fluorescently tagged dynamin to be on or near the plasma membrane, sometimes organized into discrete puncta (Figure 7). We often observed decreases in fluorescence (Figure 7, C and D), as the protein was either displaced by the fused granule membrane, or diffused into a fused granule membrane that retained curvature. Since similar decreases in fluorescence were seen for another plasma membrane-targeted probe with no known effect on secretion, this probably reflects a nonspecific consequence of localization at fusion sites (Figure S5).

Local dynamin accumulation is readily observed in clathrin-mediated endocytosis. Indeed, we detect Dyn2-GFP accumulation tens of seconds after fusion as part of the sequence of clathrin-mediated endocytosis (unpublished data). Our experiments are in agreement with two other studies with Dyn-GFP, in which dynamin accumulation was sometimes detected in the vicinity of fusion sites but only many seconds after fusion (Tsuboi *et al.*, 2002, 2004). We did not observe local accumulation of GFP-labeled dynamins immediately before or during NPY-Cherry release. It is possible that the experiments did not have the sensitivity or the temporal resolution to detect this type of change. Alternatively, dynamin action following fusion may require many fewer molecules than required for clathrin-mediated endocytosis.

Mechanistic implications

Dynamin could alter the dynamics of exocytosis through global changes in the plasma membrane/cytoplasm interface. Indeed, dynamin can induce membrane tension on lipid tubules in vitro in the presence of GTP (Roux *et al.*, 2006). In vivo, dynamin could possibly affect membrane tension through its direct and indirect interactions with the cytoskeleton (Witke *et al.*, 1998; Lee and De Camilli, 2002). However, we think this does not explain our results, since atomic force microscopy (Figure 8) did not reveal differences in surface deformability between untransfected and Dyn1(T65A)-expressing chromaffin cells. Other nonspecific effects of dynamin overexpression are also unlikely, given the opposite effects on fusion pore expansion (and endocytosis) observed with dynamin mutants with elevated and reduced GTPase activities (Dyn1(T141A) and Dyn1(T65A)). Furthermore, the similar effects of an inhibitor of dynamin GTPase activity (dynasore) and a dynamin mutant with reduced GTPase

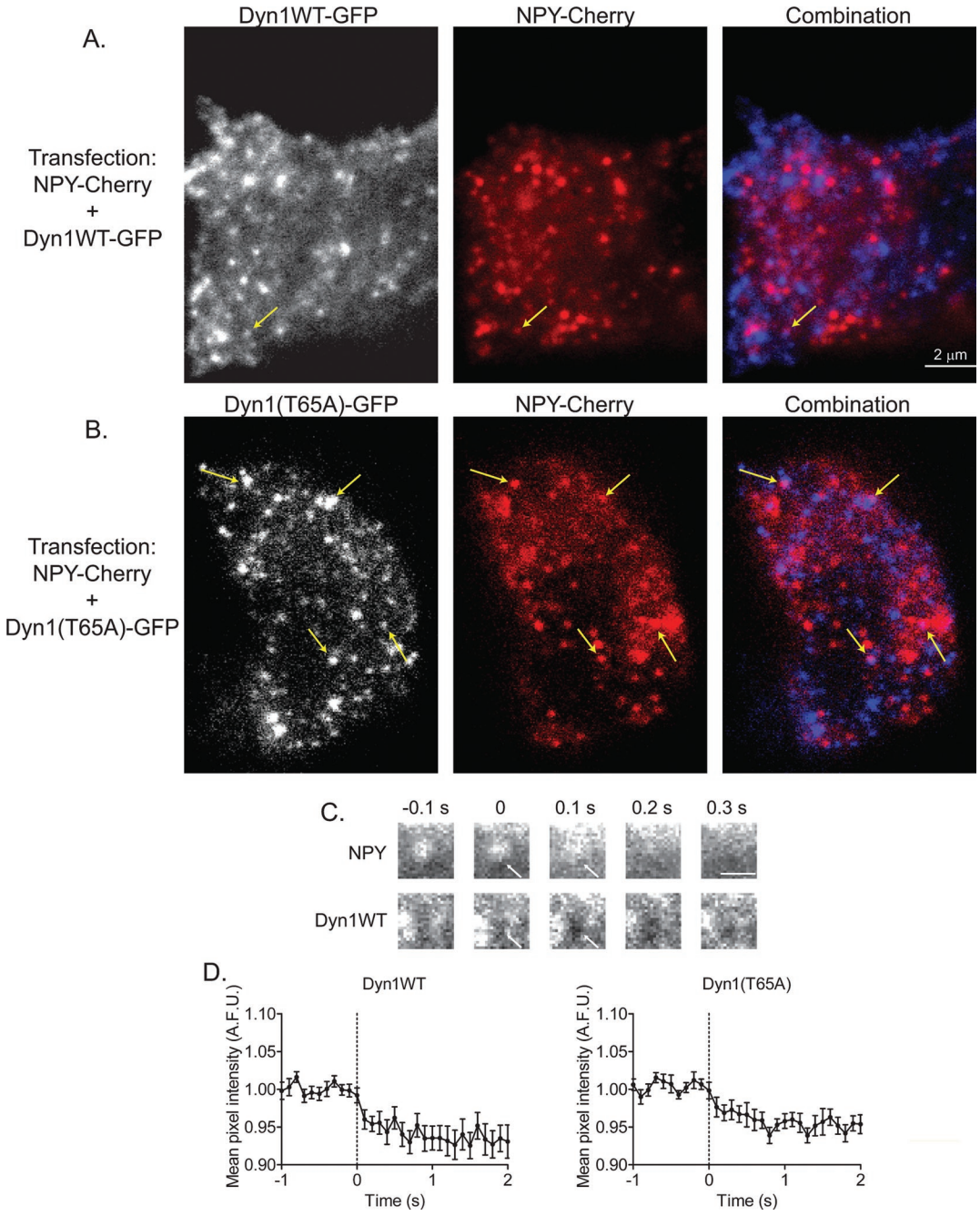

FIGURE 7: Simultaneous imaging of Dyn1-GFP and NPY-Cherry with TIRFM. (A) Chromaffin cells were cotransfected with Dyn1WT-GFP (left panel) and NPY-Cherry (middle panel); the combination image is shown in the right panel. The yellow arrow indicates an area of dynamin and granule overlap. (B) Chromaffin cells were cotransfected with Dyn1(T65A)-GFP (left) and NPY-Cherry (middle); the combination image is shown in the right panel. Yellow arrows indicate areas of dynamin and granule overlap. (C) A cell transfected with NPY-Cherry and Dyn1WT-GFP was depolarized with high extracellular K^+. A decrease in Dyn1-GFP intensity upon fusion is observed in region highlighted with arrow. (D) Dyn1WT-GFP (left) and Dyn1(T65A)-GFP (right) intensity were measured in regions of the field corresponding to granule fusion sites (ROI 292-nm radius). Dyn1WT-GFP (n = 31, 5 cells) and Dyn1(T65A)-GFP (n = 23, 7 cells) intensity values from individual fusion events were normalized to the average of 20 prefusion frames. Normalized intensities were then aligned to the prefusion frame (dotted line) and averaged (data presented as mean ± SEM).

activity (T65A), suggest that endogenous, as well as transfected, dynamin influences fusion pore expansion.

We are struck by the remarkable coherence between the current and past studies of the effects of varying dynamin's GTPase activity. Increased GTPase activity increases the rates of fusion pore expansion (Figures 2–4), rapid endocytosis (Figure S1), and slower, clathrin-mediated endocytosis (Song *et al.*, 2004). Previous studies postulating a role for dynamin in exocytosis have suggested that it is an indirect consequence of dynamin's endocytic activity, as fusion pore expansion is restricted and eventually reversed along the pathway to fission (Tsuboi *et al.*, 2004; Jaiswal *et al.*, 2009). However, it is difficult to reconcile our data with this model, especially in light of

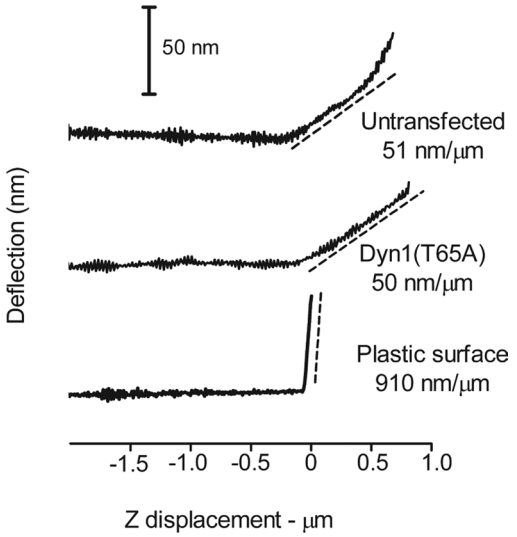

FIGURE 8: Atomic force measurements of surface elasticity of untransfected cells and cells transfected with Dyn1(T65A). Representative probe deflections during approach to (A) a nontransfected cell, (B) a cell transfected with Dyn1(T65A), and (C) the bottom of a plastic petri dish. NPY-Cherry was cotransfected with Dyn1(T65A) to detect the cell in B. Shown are the probe deflections vs. probe approach (Z) to the cell surface. The initial slopes are indicated in terms of nanometer probe deflection vs. probe approach. The spring constant of the probe was ~ 0.01 nN/m.

the finding that fusion pore expansion is actually accelerated when dynamin GTPase activity is enhanced. We favor another mechanism based upon a property of dynamin that is also essential in endocytosis: its self-limited assembly on lipids in the presence of GTP. GTP hydrolysis is enhanced manyfold by accumulation, which, in turn, reverses dynamin assembly (Warnock *et al.*, 1996; Ramachandran and Schmid, 2008) and sometimes leads to endocytosis. Membrane fission may therefore be considered a *stochastic* result of GTP hydrolysis (Bashkirov *et al.*, 2008; Pucadyil and Schmid, 2009). This notion fits well with the results in this study. We speculate that dynamin assembly restricts fusion pore expansion until GTP hydrolysis-stimulated disassembly. Higher GTPase (Dyn1(T141A)) activity causes the decision between fission or fusion pore expansion to be made earlier, with an elevated incidence of rapid endocytosis (Figure S1). Lower GTPase (Dyn1(T65A)) activity delays the decision, often stabilizing the narrow-neck fusion intermediate (Figure 2C).

Dynamin is a large multimodular protein with numerous binding partners (for a review, see Hinshaw, 2000). Thus it may not be acting alone to regulate the effects described in this study. In addition, dynamin interacts, either directly or indirectly, with several proteins that are known to be important in exocytosis, including actin (Witke *et al.*, 1998; Lee and De Camilli, 2002; Berberian *et al.*, 2009; Gu *et al.*, 2010), the SNAREs (Okamoto *et al.*, 1999; Galas *et al.*, 2000), and synaptotagmin (Robinson and Bonifacino, 2001). We suggest that dynamin's unique role in these interactions is to provide a direct biochemical link between the fusion event and membrane fission in endocytosis. Dynamin's GTPase activity controls the dynamics of its common function in these events: the shaping of local membrane curvature.

MATERIALS AND METHODS

Chromaffin cell preparation and transfection

Chromaffin cell preparation from bovine adrenal medulla and transient transfection were performed as previously described (Wick *et al.*, 1993). Cells were plated onto 25-mm coverslips (refractive index 1.51) that had been coated with poly-D-lysine and calf skin collagen to promote cell adhesion. Cells were transfected with plasmid(s) by Ca^{2+} phosphate precipitation. NPY-Cer was transfected alone or with hemagglutinin (HA)-tagged, human Dyn1 constructs (Song *et al.*, 2004) in dil experiments. The parent NPY plasmid was a gift from Wolfhard Almers (Vollum Institute, Oregon Health and Science University, Portland, OR). NPY-Cer is a soluble lumenal marker of chromaffin granules that is released upon exocytosis. Human Dyn1 WT and Dyn1 mutant coexpression with NPY-Cer was determined with immunocytochemistry. HA-tagged Dyn1 constructs were visualized with the HA-11 anti-HA antibody at a 1:200 dilution (Covance, Princeton, NJ) and Alexa Fluor 568 goat anti–mouse immunoglobulin G (IgG; Invitrogen, Carlsbad, CA) secondary antibody (1:200 dilution). There was 90% coexpression of NPY and Dyn1 in transfected chromaffin cells. Experiments were performed 3–7 d after transfection.

Perfusion

Experiments were performed in a physiological salt solution (PSS) containing 145 mM NaCl, 5.6 mM KCl, 2.2 mM $CaCl_2$, 0.5 mM $MgCl_2$, 5.6 mM glucose, 15 HEPES, pH 7.4 at ~ 28°C. Individual cells were perfused through a pipette (100 μm inner diameter) using positive pressure from a computer-controlled perfusion system DAD-6VM (ALA Scientific Instruments, Westbury, NY). Generally, cells were perfused with PSS for 5 s, and then stimulated to secrete with elevated K^+-containing solution (95 mM NaCl, 56 mM KCl, 5 mM $CaCl_2$, 0.5 mM $MgCl_2$, 5.6 mM glucose, 15 mM HEPES, pH 7.4) for 60 s. dil was added directly to cells bathed in PSS at a 1:50 dilution. The cells were then quickly washed several times in PSS and used immediately. To detect endocytosis, cells transfected with rat vesicular monoamine transporter 2–pHL (VMAT2-pHL) were perfused for 15 s with pH 7.4 elevated K^+ PSS and then exposed to pH 5.5 PSS (with MES buffer substituted for HEPES) to quench the fluorescence of extracellular-facing pHL. Bafilomycin (Amersham Biosciences, Piscataway, NJ) was added to PSS to a final concentration of 1 μM to inhibit reacidification of granules that underwent endocytosis (Fernandez-Alfonso and Ryan, 2004).

Polarized total internal reflection fluorescence microscopy

The specialized excitation system used to create the p-pol and s-pol 514-nm beams, superimpose their paths, and to further superimpose the 442-nm beam on that path is described in detail elsewhere (Anantharam *et al.*, 2010b). The system is programmed to step through a sequence of three shutter openings (one at a time for each beam), repeating the cycle without additional delay using a TTL triggering system. Objective-based TIRFM illumination was produced by directing the common beam path through a custom side port to a side-facing filter cube below the objective turret of an Olympus IX70 (inverted) microscope (Melville, NY). The filter cube contained these dichroic mirror/emission filter combinations: z442/514rpc and z442/514m for NPY-Cer/dil; and z442/561rdc and z442/561m for Dyn1-GFP/NPY-Cherry (Chroma Technology, Brattleboro, VT). The beam was focused on the periphery of the back focal plane of a 60× 1.49 NA, oil-immersion objective (Olympus) so that the laser beam was incident on the coverslip at ~70 degrees from the normal, giving a decay constant for the evanescent field of approximately 110 nm.

Concerning the emission path, a 1.5× internal magnifying lens of the Olympus microscope was used. For simultaneous imaging of GFP/Cherry, a DualView image splitter (Optical Insights, Tucson, AZ) was installed before the camera, containing dichroic mirror 560 dcxr and emission filters D510/80nm and BP620/60m (Chroma).

Approximately 1% of the emission in the GFP (short wavelength) channel resulted from direct excitation of the Cherry fluorophore. Digital images were captured on a cooled EM CCD camera (Andor iXon, Andor Technology, South Windsor, CT). The camera takes an exposure synchronous with each shutter opening. Images were acquired at ~30 Hz with 20 ms exposures and 100 gain (EM setting). At 30 Hz, the full cycle of three exposures had a period of approximately 100 ms.

Image analysis for pTIRFM

Sequential NPY-Cer, dil s-, and p-pol emission images were captured using IQ software (Andor). Normalized *P/S* ratios (see next paragraph) and *P + 2S* sums were calculated pixel by pixel for each image, and the transformations were aligned to the NPY-Cer images using custom software written in IDL (ITT, Boulder, CO). Exocytosis of individual granules was evident from the sudden and complete loss of NPY-Cer fluorescence. Changes in *P/S* and *P + 2S* were determined in a 292-nm region of interest (ROI) centered over localized increases in the *P/S* ratio at sites of exocytosis. When fusion occurred without an evident increase in *P/S*, the ROI was centered over the region of the fusing granule.

P/S varies with the relative intensities of the p- and s-pol excitations, biases in the optical system, and interference fringes. To reduce these effects and allow comparisons with theory, *P/S* data from the dil emission were normalized to the ratio obtained with solution containing 10 mM rhodamine 6G (Invitrogen), which is predicted to be randomly oriented. The normalization was performed using the spatial mean of rhodamine 6G emission excited by each of the p- and s-pol 514-nm beams. For *P + 2S*, the amplitudes of p relative to s were also corrected for by the rhodamine 6G calibration.

For the purposes of estimating noise in *P/S* and *P + 2S*, and to set a threshold above which changes are significant, the *P/S* and *P + 2S* of nonfusing granules within 3 ROIs of fusing granules was determined at the time of fusion of the neighboring granule. Changes in the *P/S* and *P + 2S* for the nonfusing granules had a standard deviation of 2% and 3%, respectively (28 granules). Changes observed near fusing granules greater than 6% were considered significant.

Amperometry

Perfusion solutions and conditions were identical to those used for imaging experiments. Chromaffin cells were transfected with NPY-GFP (to visualize granules) alone or with human Dyn1 constructs. Carbon-fiber electrodes (5 µm; ALA Scientific, Westbury, NY) were held at + 650 mV and positioned so that they touched the membrane of cells expressing fluorescent protein. Secretion was stimulated via local application of 56 mM K^+ for 60 s. Currents were collected using an Axopatch 200 A amplifier modified for extended voltage output (Axon Instruments, Foster City, CA), filtered at 2 kHz, and sampled at 4 kHz (Lam *et al.*, 2008; Anantharam *et al.*, 2010b). No digital filtering was applied. Currents were analyzed using an IGOR XOP (Wavemetrics, Portland, OR; Mosharov and Sulzer, 2005). Only spikes with amplitudes greater than 10 pA and rise times less than 5 ms were used in the spike analysis. PSF analysis was limited only to those PSFs with amplitudes greater than 1 pA and durations greater than 2.5 ms. To obtain a measure for the fusion pore open time, we followed the analysis of Meyer Jackson and colleagues (Wang *et al.*, 2001). Because the transitions of fusion pores are stochastic (like ion channels), lifetime distributions were used to characterize their kinetics. The distributions were fit well by single exponentials (r^2 = 0.99), with time constants equal to the mean open time.

Confocal microscopy

Images of transfected cells displaying fluorescent signals were acquired on an Olympus Fluoview 500 confocal microscope with a 60× 1.42 NA oil objective. For imaging, an argon 488-nm laser with a 505- to 525-nm bandpass filter, an HeNe green 543-nm laser with a 560- to 600-nm bandpass filter, and a HeNe red (633-nm) laser with a longpass filter were used. Images were analyzed with ImageJ software (http://rsb.info.nih.gov/ij/download.html), and statistics were performed with Prism 5 software from Graphpad Prism Software (La Jolla, CA).

Immunocytochemistry

Chromaffin cells were plated on Lab-Tek II chambered coverslips (Nalge Nunc International, distributed by Thermo Fisher Scientific, Rochester, NY) that had been sequentially coated with poly-D-lysine and calf skin collagen to promote cell adhesion. Cells were cotransfected with NPY-Cherry and HA-tagged Dyn1 constructs. Four or five days after transfection, cells were fixed in glutaraldehyde, followed by permeabilization with methanol and exposure to antibodies. NPY was visualized directly by the intrinsic fluorescence of the Cherry fluorophore. For confocal imaging (Figures 6, 7, and S4), HA-tagged Dyn1 constructs were visualized with a goat polyclonal anti-HA antibody (GenScript A00168, 1:200 dilution) and Alexa Fluor 647 donkey anti–goat IgG (Invitrogen/Molecular Probes) secondary antibody (1:300 dilution). Both endogenous dynamin 1 and the HA-tagged constructs were detected with a monoclonal anti-dynamin 1 antibody (Hudy 1, 1:100 dilution; Millipore, Billerica, MA) followed by Alexa Fluor 488 donkey anti–mouse IgG (1:300 dilution; Invitrogen/Molecular Probes).

Atomic Force Microscopy

Atomic force microscopy was used to measure surface elasticity of chromaffin cells with and without transfected Dyn1(T65A). Measurements were performed on a BioScope Catalyst Life Science Atomic Force Microscope (Veeco/Bruker Nano, Santa Barbara, CA) equipped with fluorescence imaging. Transfected chromaffin cells were detected by the presence of NPY-Cherry fluorescent secretory granules. Chromaffin cells are approximately 15-µm diameter, round cells; measurements were readily performed away from the edges of cells to minimize the influence of the glass substrate on surface measurements. An MLCT probe was used with a 20-nm diameter and a spring constant of ~0.01 N/m. Tip deflections versus Z-distance curves were taken at user-defined locations under bright-field and fluorescence illumination. The maximum load on the cell surface was less than 1 nN to prevent damage to the cells. Multiple curves were taken at different locations on the same cell.

ACKNOWLEDGMENTS

We thank Paul Jenkins, Lian Zhang, and Jeffrey Martens for help in preparing some of the plasmid reagents and Widmann W. Hoerauf for assistance with amperometry. We are indebted to Andrea Slade of Veeco/Bruker Nano for the atomic force microscopy measurements. This work was supported by NIH grant R01-NS38129 to R.W.H. and D.A., NIH grants MH61345 and GM42455 to S.L.S., NIH grants R01-NS053978 and DK077050 to E.L.S., and NIH fellowships T32DA007268 and F32GM086169 to A.A. This work benefited from a subsidy for DNA sequencing from the University of Michigan Comprehensive Cancer Center.

REFERENCES

Albillos A, Dernick G, Horstmann H, Almers W, Alvarez de Toledo G, Lindau M (1997). The exocytotic event in chromaffin cells revealed by patch amperometry. Nature 389, 509–512.

Anantharam A, Axelrod D, Holz RW (2010a). Polarized TIRFM reveals changes in plasma membrane topology before and during granule fusion. Cell Mol Neurobiol 30, 1343–1349.
Anantharam A, Onoa B, Edwards RH, Holz RW, Axelrod D (2010b). Localized topological changes of the plasma membrane upon exocytosis visualized by polarized TIRFM. J Cell Biol 188, 415–428.
Artalejo CR, Elhamdani A, Palfrey HC (2002). Sustained stimulation shifts the mechanism of endocytosis from dynamin-1-dependent rapid endocytosis to clathrin- and dynamin-2-mediated slow endocytosis in chromaffin cells. Proc Natl Acad Sci USA 99, 6358–6363.
Artalejo CR, Henley JR, McNivan MA, Palfrey HC (1995). Rapid endocytosis coupled to exocytosis in adrenal chromaffin cells involves Ca2+, GTP, and dynamin but not clathrin. Proc Natl Acad Sci USA 92, 8328–8332.
Bashkirov PV, Akimov SA, Evseev AI, Schmid SL, Zimmerberg J, Frolov VA (2008). GTPase Cycle of dynamin is coupled to membrane squeeze and release, leading to spontaneous fission. Cell 135, 1276–1286.
Berberian K, Torres AJ, Fang Q, Kisler K, Lindau M (2009). F-actin and myosin II accelerate catecholamine release from chromaffin granules. J Neurosci 29, 863–870.
Chow RH, von Ruden L, Neher E (1992). Delay in vesicle fusion revealed by electrochemical monitoring of single secretory events in adrenal chromaffin cells. Nature 356, 60–63.
Damke H, Baba T, Warnock DE, Schmid SL (1994). Induction of mutant dynamin specifically blocks endocytic coated vesicle formation. J Cell Biol 127, 915–934.
Doherty GJ, McMahon HT (2009). Mechanisms of endocytosis. Annu Rev Biochem 78, 857–902.
Fernandez-Alfonso T, Ryan TA (2004). The kinetics of synaptic vesicle pool depletion at CNS synaptic terminals. Neuron 41, 943–953.
Fulop T, Doreian B, Smith C (2008). Dynamin I plays dual roles in the activity-dependent shift in exocytic mode in mouse adrenal chromaffin cells. Arch Biochem Biophys 477, 146–154.
Fulop T, Radabaugh S, Smith C (2005). Activity-dependent differential transmitter release in mouse adrenal chromaffin cells. J Neurosci 25, 7324–7332.
Galas MC, Chasserot-Golaz S, Dirrig-Grosch S, Bader MF (2000). Presence of dynamin–syntaxin complexes associated with secretory granules in adrenal chromaffin cells. J Neurochem 75, 1511–9.
Gonzalez-Jamett AM, Baez-Matus X, Hevia MA, Guerra MJ, Olivares MJ, Martinez AD, Neely A, Cardenas AM (2010). The association of dynamin with synaptophysin regulates quantal size and duration of exocytotic events in chromaffin cells. J Neurosci 30, 10683–10691.
Graham ME, O'Callaghan DW, McMahon HT, Burgoyne RD (2002). Dynamin-dependent and dynamin-independent processes contribute to the regulation of single vesicle release kinetics and quantal size. Proc Natl Acad Sci USA 99, 7124–7129.
Gu C, Yaddanapudi S, Weins A, Osborn T, Reiser J, Pollak M, Hartwig J, Sever S (2010). Direct dynamin-actin interactions regulate the actin cytoskeleton. EMBO J 29, 3593–3606.
Henkel AW, Almers W (1996). Fast steps in exocytosis and endocytosis studied by capacitance measurements in endocrine cells. Curr Opin Neurobiol 6, 350–357.
Hinshaw JE (2000). Dynamin and its role in membrane fission. Annu Rev Cell Dev Biol 16, 483–519.
Hinshaw JE, Schmid SL (1995). Dynamin self-assembles into rings suggesting a mechanism for coated vesicle budding. Nature 374, 190–192.
Holroyd P, Lang T, Wenzel D, De Camilli P, Jahn R (2002). Imaging direct, dynamin-dependent recapture of fusing secretory granules on plasma membrane lawns from PC12 cells. Proc Natl Acad Sci USA 99, 16806–16811.
Jaiswal JK, Rivera VM, Simon SM (2009). Exocytosis of post-Golgi vesicles is regulated by components of the endocytic machinery. Cell 137, 1308–1319.
Lam AD, Tryoen-Toth P, Tsai B, Vitale N, Stuenkel EL (2008). SNARE-catalyzed fusion events are regulated by syntaxin1A-lipid interactions. Mol Biol Cell 19, 485–497.
Lee E, De Camilli P (2002). Dynamin at actin tails. Proc Natl Acad Sci USA 99, 161–166.
Liu YW, Surka MC, Schroeter T, Lukiyanchuk V, Schmid SL (2008). Isoform and splice-variant specific functions of dynamin-2 revealed by analysis of conditional knock-out cells. Mol Biol Cell 19, 5347–5359.
Macia E, Ehrlich M, Massol R, Boucrot E, Brunner C, Kirchhausen T (2006). Dynasore, a cell-permeable inhibitor of dynamin. Dev Cell 10, 839–850.
Marks B, Stowell MHB, Vallis Y, Mills IG, Gibson A, Hopkins CR, McMahon HT (2001). GTPase activity of dynamin and resulting conformation change are essential for endocytosis. Nature 410, 231–235.
Mosharov EV, Sulzer D (2005). Analysis of exocytotic events recorded by amperometry. Nat Methods 2, 651–658.
Newton AJ, Kirchhausen T, Murthy VN (2006). Inhibition of dynamin completely blocks compensatory synaptic vesicle endocytosis. Proc Natl Acad Sci USA 103, 17955–17960.
Okamoto M, Schoch S, Sudhof TC (1999). EHSH1/intersectin, a protein that contains EH and SH3 domains and binds to dynamin and SNAP-25. A protein connection between exocytosis and endocytosis? J Biol Chem 274, 18446–18454.
Onoa B, Li H, Gagnon-Bartsch JA, Elias LA, Edwards RH (2010). Vesicular monoamine and glutamate transporters select distinct synaptic vesicle recycling pathways. J Neurosci 30, 7917–7927.
Perrais D, Kleppe IC, Taraska JW, Almers W (2004). Recapture after exocytosis causes differential retention of protein in granules of bovine chromaffin cells. J Physiol 560, 413–428.
Pucadyil TJ, Schmid SL (2009). Conserved functions of membrane active GTPases in coated vesicle formation. Science 325, 1217–1220.
Ramachandran R, Schmid SL (2008). Real-time detection reveals that effectors couple dynamin's GTP-dependent conformational changes to the membrane. EMBO J 27, 27–37.
Robinson MS, Bonifacino JS (2001). Adaptor-related proteins. Curr Opin Cell Biol 13, 444–453.
Roux A, Uyhazi K, Frost A, De Camilli P (2006). GTP-dependent twisting of dynamin implicates constriction and tension in membrane fission. Nature 441, 528–531.
Song BD, Leonard M, Schmid SL (2004). Dynamin GTPase domain mutants that differentially affect GTP binding, GTP hydrolysis, and clathrin-mediated endocytosis. J Biol Chem 279, 40431–40436.
Takei K, McPherson PS, Schmid SL, De Camilli P (1995). Tubular membrane invaginations coated by dynamin rings are induced by GTP-gamma S in nerve terminals. Nature 374, 186–190.
Taraska JW, Perrais D, Ohara-Imaizumi M, Nagamatsu S, Almers W (2003). Secretory granules are recaptured largely intact after stimulated exocytosis in cultured endocrine cells. Proc Natl Acad Sci USA 100, 2070–2075.
Tsuboi T, McMahon HT, Rutter GA (2004). Mechanisms of dense core vesicle recapture following "kiss and run" ("cavicapture") exocytosis in insulin-secreting cells. J Biol Chem 279, 47115–47124.
Tsuboi T, Terakawa S, Scalettar BA, Fantus C, Roder J, Jeromin A (2002). Sweeping model of dynamin activity. Visualization of coupling between exocytosis and endocytosis under an evanescent wave microscope with green fluorescent proteins. J Biol Chem. 277, 15957–15961.
Wang L, Bittner MA, Axelrod D, Holz RW (2008). The structural and functional implications of linked SNARE motifs in SNAP25. Mol Biol Cell 19, 3944–3955.
Wang CT, Grishanin R, Earles CA, Chang PY, Martin TFJ, Chapman ER, Jackson MB (2001). Synaptotagmin modulation of fusion pore kinetics in regulated exocytosis of dense-core vesicles. Science 294, 1111–1115.
Warnock DE, Baba T, Schmid SL (1997). Ubiquitously expressed dynamin-II has a higher intrinsic GTPase activity and a greater propensity for self-assembly than neuronal dynamin-I. Mol Biol Cell 8, 2553–2562.
Warnock DE, Hinshaw JE, Schmid SL (1996). Dynamin self-assembly stimulates its GTPase activity. J Biol Chem 271, 22310–22314.
Warnock DE, Terlecky LJ, Schmid SL (1995). Dynamin GTPase is stimulated by crosslinking through the C-terminal proline-rich domain. EMBO J 14, 1322–1328.
Wick PW, Senter RA, Parsels LA, Holz RW (1993). Transient transfection studies of secretion in bovine chromaffin cells and PC12 cells: generation of kainate-sensitive chromaffin cells. J Biol Chem 268, 10983–10989.
Wightman RM, Jankowski JA, Kennedy RT, Kawagoe KT, Schroeder TJ, Leszczyszyn DJ, Near JA, Diliberto EJ Jr., Viveros OH (1991). Temporally resolved catecholamine spikes correspond to single vesicle release from individual chromaffin cells. Proc Natl Acad Sci USA 88, 10754–10758.
Witke W, Podtelejnikov AV, Di Nardo A, Sutherland JD, Gurniak CB, Dotti C, Mann M (1998). In mouse brain profilin I and profilin II associate with regulators of the endocytic pathway and actin assembly. EMBO J 17, 967–976.
Zhou Z, Misler S, Chow RH (1996). Rapid fluctuations in transmitter release from single vesicles in bovine adrenal chromaffin cells. Biophys J 70, 1543–1552.